INORGANIC CHEMISTRY FRONTIERS

RESEARCH ARTICLE

View Article Online
View Journal | View Issue

Cite this: *Inorg. Chem. Front.*, 2025, **12**, 4712

$Hg_2(HTe_2O_5)(PO_4)$: a novel phosphate crystal with enhanced birefringence enabled by the synergistic modification of multiple functional groups†

Peng-Fei Li, [a,b,c] Chun-Li Hu,*[a,c] Bo Zhang, [a,b,c] Jiang-Gao Mao [a,c] and Fang Kong *[a,b,c]

Birefringent crystals are crucial for the miniaturization of optical devices. Phosphate crystals, characterized by their highly symmetrical tetrahedral structures, exhibit excellent stability and wide optical bandgaps. However, their intrinsic symmetry typically results in low birefringence, with most phosphate compounds having birefringence values below 0.1. Efforts to enhance birefringence by introducing highly anisotropic ions and groups have been impeded by the tetrahedral coordination of phosphate, which often leads to the cancellation of anisotropic effects. To address this challenge, we propose an approach that leverages the synergistic modification of multiple functional groups to disrupt the anisotropic cancellation in phosphate crystals and significantly enhance their birefringence. Specifically, we incorporate Te(IV), which features stereo-chemically active lone pairs, and Hg(II), known for its high polarizability and deformability, into the phosphate system. We synthesized a novel phosphate compound, $Hg_2(HTe_2O_5)(PO_4)$, which exhibits a calculated birefringence of 0.162 at 546 nm and a measured birefringence of 0.168 at 546 nm. This value is comparable to that of the commercial birefringent material $CaCO_3$ (Δn = 0.172@546 nm) and surpasses most previously reported phosphate materials. Additionally, $Hg_2(HTe_2O_5)(PO_4)$ demonstrates a wide bandgap and excellent stability. Using the PAWED method, we determined that the significant birefringence of $Hg_2(HTe_2O_5)(PO_4)$ is primarily due to the combined contributions of the HgO_7 polyhedra (19.86%), PO_4 tetrahedra (29.17%), and Te_2O_5 groups (47.40%). Our work demonstrates that the synergistic modification of multiple functional groups is an effective strategy for enhancing the birefringence of tetrahedral compounds, providing a new pathway for the development of high-performance birefringent materials.

Received 15th March 2025,
Accepted 12th April 2025

DOI: 10.1039/d5qi00757g

rsc.li/frontiers-inorganic

Introduction

Tetrahedral phosphate crystals have received significant attention in the design of optical functional crystals due to their excellent thermal stability and short ultraviolet cutoff edges.[1–4] Among them, typical compounds such as KH_2PO_4 (KDP) and $KTiOPO_4$ (KTP) have been successfully commercialized as nonlinear optical crystals.[5] However, the highly symmetrical tetrahedral configuration of phosphate crystals generally results in low birefringence, which poses a considerable barrier to the miniaturization of optical devices.[6–11] Therefore, enhancing the birefringence of phosphate materials has become an urgent and critical issue.

To enhance the birefringence of phosphates, researchers have made efforts in several aspects: (i) combining with π-conjugated groups,[12–14] such as $K_2PbB_5P_3O_{17}$ (0.045@1064 nm),[15] $Cs_3[(BOP)_2(B_3O_7)_3]$ (0.075@532 nm),[16] $K_3B_4PO_{10}$ (0.0445@532 nm)[17] and $(NH_4)_3B_{11}PO_{19}F_3$ (0.045@1064 nm);[18] (ii) introducing d^{10} transition metals with high polarizability,[19,20] such as $Na(C_2H_{10}N_2)_2[Zn_3(PO_4)_2(H_{0.5}PO_4)]_2$ (0.060@546 nm),[21] $(NH_4)_3(H_3O)Zn_4(PO_4)_4$ (0.032@1064 nm),[22] and $LiHgPO_4$ (0.068@1064 nm);[23] (iii) incorporating lone-pair cations,[24–28] for example, $(NH_4)_3[Sn_2(PO_4)_2]Cl$ (0.065@1064 nm),[29] $Cs_2Sb_3O(PO_4)_3$ (0.034@1064 nm),[30] $[Sn_3OF]PO_4$ (0.104@546 nm),[31] $SrSn(PO_4)PO_2(OH)_2$ (0.080@1064 nm),[32] Sn_2PO_4I (0.664@546 nm),[33] $Ba_2TeP_2O_9$ (0.126@1064 nm),[34] $Rb_2SbFP_2O_7$ (0.15@546 nm)[35] and α-$NaSb_3P_2O_{10}$ (0.121@1064 nm);[36] (iv) adding d^0 transition metal cations,[37,38] like $[C(NH_2)_3]_{10}(MoO_3)_{10}(PO_4)_2(HPO_4)_2{\cdot}5H_2O$

[a]*State Key Laboratory of Functional Crystals and Devices, Fujian Institute of Research on the Structure of Matter, Chinese Academy of Sciences, Fuzhou 350002, P. R. China. E-mail: clhu@fjirsm.ac.cn, kongfang@fjirsm.ac.cn*
[b]*College of Chemistry, Fuzhou University, Fuzhou 350108, P. R. China*
[c]*University of Chinese Academy of Sciences, Beijing 100049, P. R. China*

†Electronic supplementary information (ESI) available: Experimental section, computational method, crystal data, important bond distances and bond valences, PXRD patterns, TGA curves, IR spectrum, experimental birefringence and band structures. CCDC 2430737. For ESI and crystallographic data in CIF or other electronic format see DOI: https://doi.org/10.1039/d5qi00757g

(0.158@550 nm),[39] $LiTiOPO_4$ (0.17@1064 nm)[40] and $K_2MgMoP_2O_{10}$ (0.187@546 nm).[41] Although the introduction of these highly anisotropic ions and groups has to some extent improved the birefringence of phosphates, the highly symmetrical tetrahedral configuration inevitably leads to the cancellation of polarization anisotropy, resulting in most compounds having birefringence values below 0.1.

To address this challenge, we propose a strategy of synergistic modification using multiple functional groups to enhance the birefringence of phosphates. First, different functional groups exhibit varying degrees of polarization anisotropy, which can prevent the complete cancellation of polarization anisotropy when coordinated with phosphate groups. Moreover, the interactions between different functional groups can avoid their coordination with phosphate in a regular tetrahedral form. Therefore, we attempt to introduce multiple functional groups to improve the birefringence of phosphates.

The d^{10} transition metal Hg features diverse coordination configurations, high polarizability, and deformability, all of which positively contribute to birefringence.[42–44] Meanwhile, Te(IV) with lone-pair electrons also possesses strong anisotropy, which is beneficial for enhancing the birefringence of compounds.[45–48] More importantly, our previous work in Hg-based and Te-based birefringent materials has yielded fruitful results, successfully pushing the birefringence of sulfates to 0.542 at 546 nm.[49] To obtain phosphate materials with large birefringence, we attempt to combine the above two groups with phosphates. We have conducted research in the Hg–Te–P–O system and successfully synthesized $Hg_2(HTe_2O_5)(PO_4)$. This compound exhibits a large birefringence of 0.162 at 546 nm, a wide bandgap of 3.58 eV, and excellent stability. This paper will introduce its synthesis, structure, optical properties, and theoretical calculations.

Results and discussion

Compound $Hg_2(HTe_2O_5)(PO_4)$ was successfully synthesized *via* a conventional hydrothermal method using TeO_2, HgO, and H_3PO_3 as starting materials at 230 °C, yielding a product with a 36% yield. Detailed synthetic procedures can be found in the "Synthesis" section of the ESI.† The purity of the $Hg_2(HTe_2O_5)(PO_4)$ was confirmed by powder X-ray diffraction (XRD), as shown in Fig. S1.† Detailed crystallographic information is provided in Table S1 of the ESI.†

$Hg_2(HTe_2O_5)(PO_4)$ crystallizes in the triclinic space group $P\bar{1}$ with the following unit cell parameters: a = 5.8856(3) Å, b = 7.2589(3) Å, c = 10.1972(4) Å, α = 81.006(3)°, β = 74.483(3)°, γ = 82.959(4)°, and V = 413.12(3) Å^3. The asymmetric unit consists of two Hg atoms, two Te atoms, one P atom, one H atom, and nine O atoms, comprising a total of fifteen atoms, all of which are located in general positions. In this structure, each P atom is tetrahedrally coordinated to four O atoms, with P–O bond lengths ranging from 1.539(6) to 1.560(6) Å. The Te atoms are coordinated to three O atoms in a trigonal pyramidal geometry, with Te–O bond lengths ranging from 1.870(6) to 1.999(5) Å. The Hg atoms are coordinated to seven O atoms, forming a HgO_7 polyhedron, with Hg–O bond lengths ranging from 2.108(6) to 2.805(5) Å. Bond valence calculations reveal that the bond valences of Hg, Te, and P are 2.047–2.139, 3.461–3.536, and 4.696, respectively, indicating oxidation states of +2, +4, and +5. The lower oxidation state of Te may be attributed to the neglect of Te–O bonds longer than 2.0 Å. If these bonds are considered, the oxidation states of Te(1) and Te(2) can be increased to 4.176 and 3.802, respectively.

$Hg_2(HTe_2O_5)(PO_4)$ exhibits a three-dimensional (3D) structure composed of two-dimensional (2D) mercury tellurite layers bridged by phosphate tetrahedra (Fig. 1). Within this structure, two $Hg(1)O_7$ polyhedra share oxygen atoms to form $Hg(1)_2O_{12}$ dimers, which are further interconnected with two $Hg(2)O_7$ polyhedra to create a mercuric oxide six-membered ring as the fundamental building unit (Fig. 1a). These six-membered rings extend to form a 2D mercury oxide layer (Fig. 1d). The Te_2O_5 units are connected to this layer through oxygen atoms O(1), O(2), O(3), O(4) and O(5), thereby constructing the mercury tellurite layers (Fig. 1c). The phosphate tetrahedra bridge these layers by linking four oxygen atoms to two Hg(1) and two Hg(2) atoms (Fig. 1b), ultimately forming the 3D network structure of the compound (Fig. 1e).

Thermogravimetric analysis (TGA) of $Hg_2(HTe_2O_5)(PO_4)$ was investigated under a N_2 atmosphere over a temperature range of 20 to 1200 °C (Fig. S2†). The compound was found to be stable up to 300 °C. Upon heating to 1200 °C, the compound exhibited a weight loss equivalent to the release of 0.5 molecules of H_2O, 2 molecules of Hg, and 1 molecule of TeO_2. The experimental weight loss was 87.9%, which is in good agreement with the calculated theoretical value of 87.6%. Additionally, the compound was exposed to air for up to six months and remained stable throughout the exposure period, indicating its robustness under atmospheric conditions.

The infrared spectrum (IR) $Hg_2(HTe_2O_5)(PO_4)$ was performed using KBr as a background at room temperature (Fig. S3†). The results revealed distinct absorption peaks at 3459 cm^{-1}, 1651 cm^{-1} and 1602 cm^{-1}, which are attributed to the vibrational absorption of O–H bonds. Additionally, absorption peaks at 990 cm^{-1}, 1083 cm^{-1}, and 1352 cm^{-1} correspond to the asymmetric and symmetric stretching vibrations of P–O bonds. Peaks in the range of 777–860 cm^{-1} and 535 cm^{-1} are associated with the symmetric stretching and bending vibrations of P–O bonds. The absorption peaks for Te–O bonds appear in the ranges of 459–535 cm^{-1} and 615–674 cm^{-1}. These observed peaks are consistent with those reported in the literature. Compared with the IR spectrum of the compound $Hg_2^{I}Hg^{II}(Te_2O_4)_2(HPO_4)_2$, $Hg_2(HTe_2O_5)(PO_4)$ does not show the characteristic P–H peaks around 2350 cm^{-1}, which further confirms the correctness of the hydrogen addition in our structural analysis.[50] Additionally, the assignments of these absorption peaks are consistent with those reported in the literature.[51–54]

The UV–Vis–NIR spectrum of $Hg_2(HTe_2O_5)(PO_4)$ was measured in the range of 2000 to 200 nm (Fig. 2). The results show that the UV cutoff edge of this compound is at 282 nm,

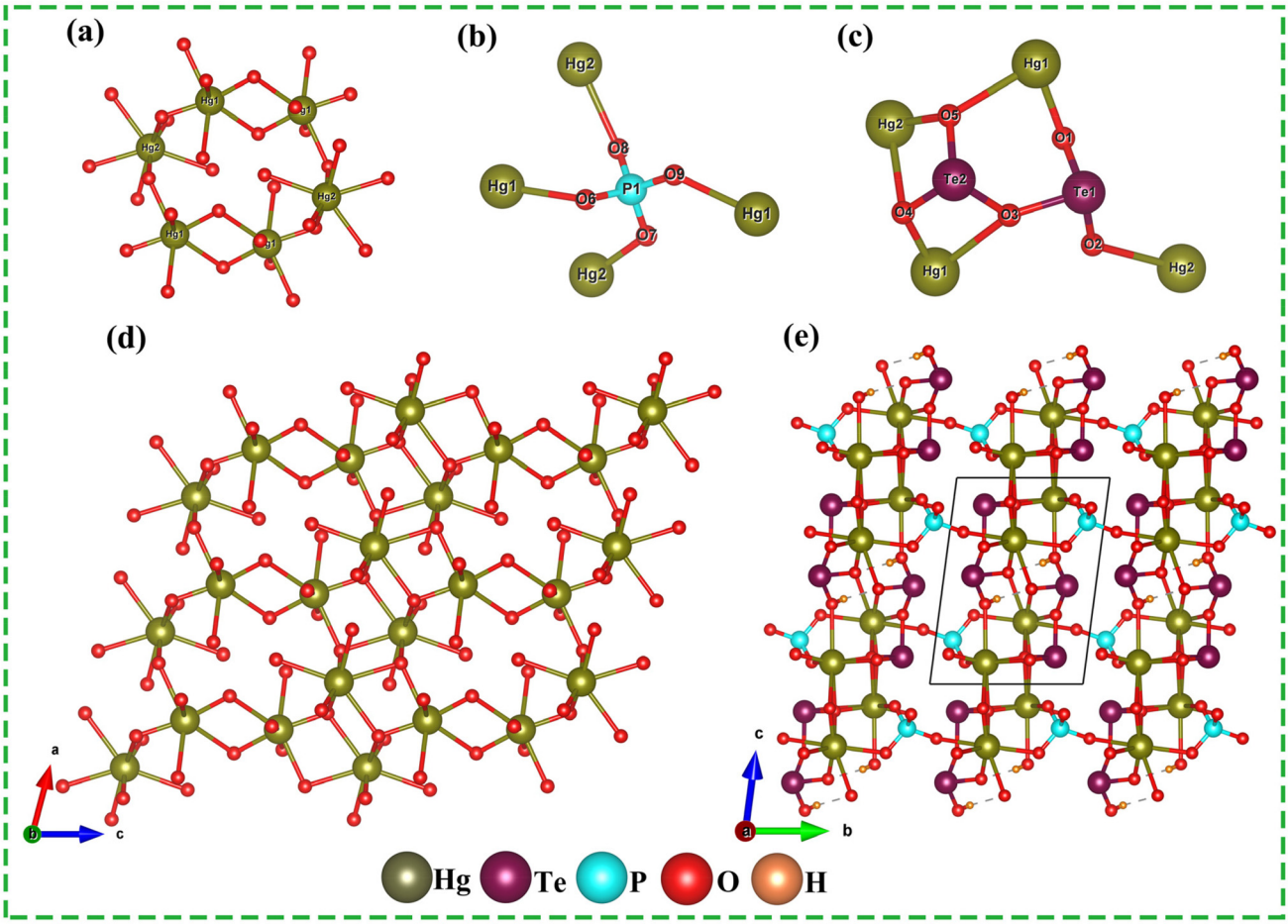

Fig. 1 Mercuric oxide six-membered ring (a), the coordination environments of PO_4 group (b), the coordination environments of Te_2O_5 group (c), two-dimensional layer structure of mercury oxide (d) and three-dimensional structure of $Hg_2(HTe_2O_5)(PO_4)$ (e).

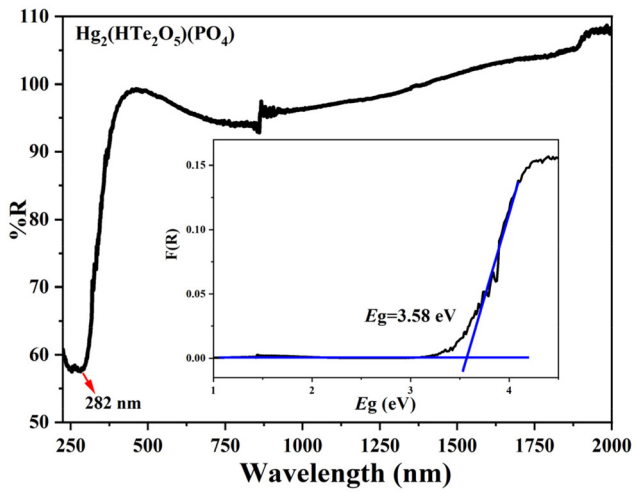

Fig. 2 The UV–Vis–NIR diffuse reflectance spectra of $Hg_2(HTe_2O_5)(PO_4)$.

corresponding to an experimental band gap of 3.58 eV. This band gap is comparable to or even larger than those of previously reported Hg-based compounds, such as $Hg_2(SeO_3)(TeO_3)$ (3.5 eV),[55] $Hg_3Se(SeO_3)(SO_4)$ (3.5 eV),[42] $Rb_2Hg_2(SeO_3)$ (3.6 eV),[56] $Hg_3(Te_3O_8)(SO_4)$ (3.36 eV)[57] and $Hg_2Ga(SeO_3)_2F$ (2.8 eV).[58]

In Fig. S4,† the birefringence of $Hg_2(HTe_2O_5)(PO_4)$ was measured at 546 nm using a polarizing microscope. $Hg_2(HTe_2O_5)(PO_4)$ exhibited complete extinction under positive polarization. The optical path difference was observed to be 0.954 μm for a crystal thickness of 5.67 μm. By employing the formula $R = \Delta n \times T$ (where R represents the optical path difference, Δn is the birefringence, and T is the thickness),[59] the experimental birefringence of $Hg_2(HTe_2O_5)(PO_4)$ at 546 nm was determined to be 0.168.

To gain a deeper understanding of the relationship between the structure and optical properties, we employed density functional theory (DFT) to investigate the electronic structure and linear optical properties of $Hg_2(HTe_2O_5)(PO_4)$. The calculations reveal that $Hg_2(HTe_2O_5)(PO_4)$ is an indirect bandgap material with a theoretical bandgap of 2.755 eV (Fig. S5†). Due to the limitations of the GGA-PBE functional, the theoretical bandgap is underestimated.[60–62] To reduce the computational error, we subsequently applied a scissor operator of 0.825 eV in our calculations. The total and partial density of states

(DOS) diagrams show that the valence band maximum of $Hg_2(HTe_2O_5)(PO_4)$ is primarily composed of O-2p orbitals, while the conduction band minimum is mainly contributed by Te-5p and Hg-6s orbitals. Therefore, the bandgap of this compound is predominantly determined by the O, Te, and Hg atoms (Fig. 3).

The linear optical response properties of $Hg_2(HTe_2O_5)(PO_4)$ were calculated based on the complex dielectric function $\varepsilon(\omega) = \varepsilon_1(\omega) + i\varepsilon_2(\omega)$ (Fig. 4).[63] This compound is a biaxial crystal and exhibits different refractive indices along the x, y, and z axes. The calculations show that the birefringence of this compound is 0.162 at 546 nm and 0.147 at 1064 nm, which is close to the measured birefringence of 0.168 at 546 nm. Through the synergistic modification of multiple functional groups, we successfully increased the birefringence of the phosphate material to above 0.1, reaching a level comparable to that of the commercial birefringent crystal $CaCO_3$ (0.172@546 nm).[64] The birefringence of this compound is significantly higher than that of some previously reported phosphate birefringent materials, such as $LiHgPO_4$ (0.068@1064 nm)[23] and $SnHPO_4$ (0.078@550 nm).[65] Excitingly, the birefringence of $Hg_2(HTe_2O_5)(PO_4)$ even surpasses that of some lone-pair systems, such as $Hg_2(SeO_3)(TeO_3)$ (0.097@546 nm),[55] $Cs_2Hg_3(SeO_3)_4$ (0.043@546 nm),[56] $Sb_4O_5I_2$ (0.084@1064 nm),[66] $Rb_3Sb_2OCl_7$ (0.098@1064 nm)[67] and $AgAl(Te_4O_{10})$ (0.092@1064 nm).[68]

To further elucidate the origin of the large birefringence in $Hg_2(HTe_2O_5)(PO_4)$, we conducted an analysis using the Polarizability Anisotropy Weighted Electron Density (PAWED) method (Fig. 5).[69] Our findings indicate that the significant birefringence of $Hg_2(HTe_2O_5)(PO_4)$ is primarily attributed to the synergistic contributions from the HgO_7 polyhedra, Te_2O_5 groups, and PO_4 tetrahedra. Specifically, the contributions from these structural units are 19.86%, 47.40%, and 29.17%, respectively. This suggests that the HgO_7 polyhedra, Te_2O_5 groups, and PO_4 tetrahedra play a dominant role in the birefringence, with the Te_2O_5 groups contributing the most.

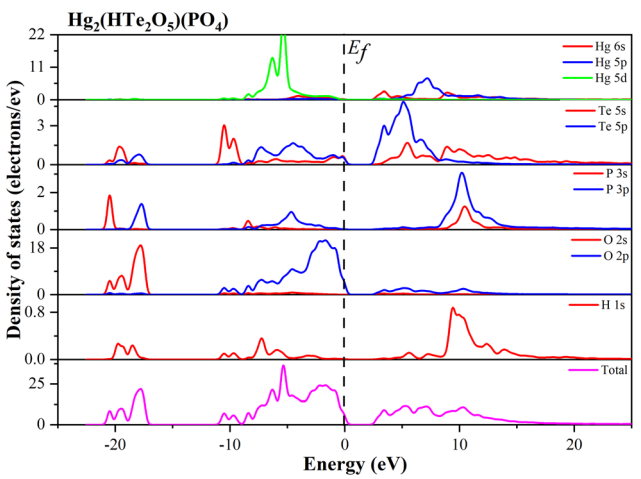

Fig. 3 The total and partial density of states for $Hg_2(HTe_2O_5)(PO_4)$.

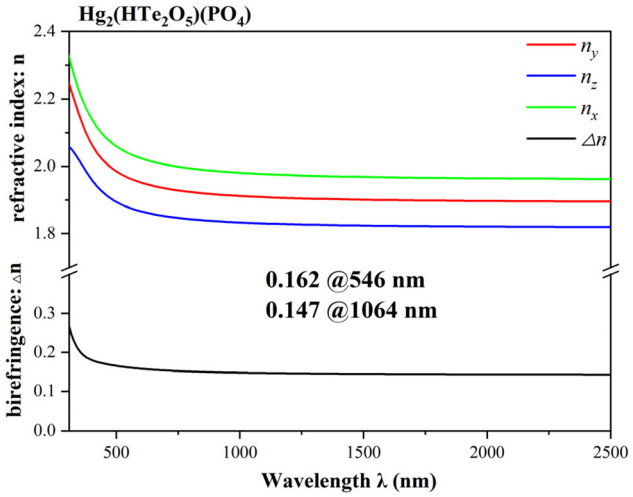

Fig. 4 The calculated refractive indices and birefringence values of $Hg_2(HTe_2O_5)(PO_4)$.

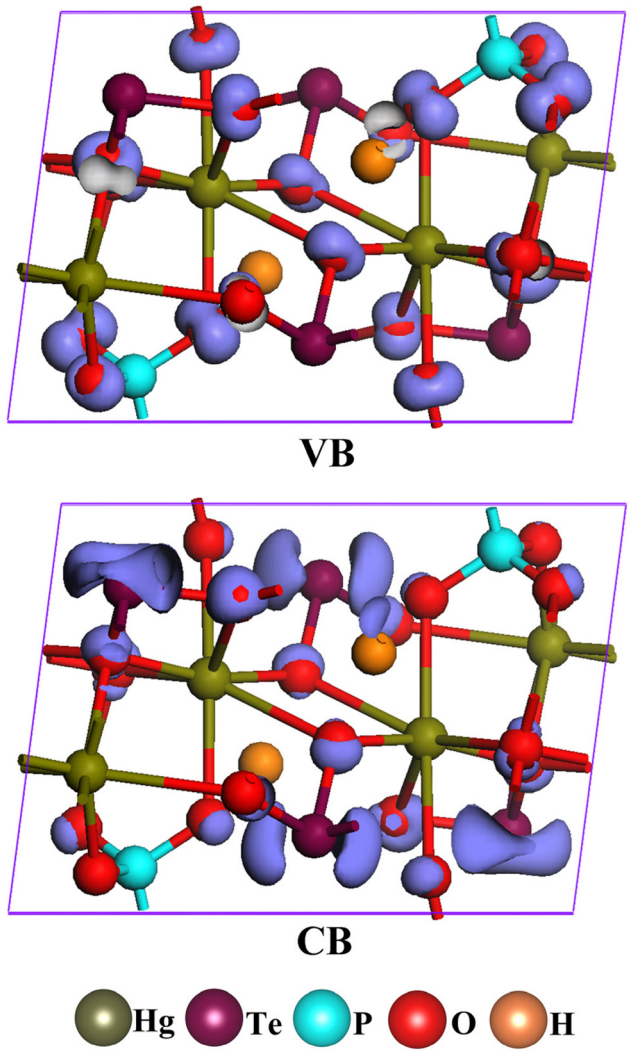

Fig. 5 PAWED plots in the VB and CB for $Hg_2(HTe_2O_5)(PO_4)$.

Conclusions

In summary, we have successfully synthesized the phosphate tellurite compound $Hg_2(HTe_2O_5)(PO_4)$ *via* a hydrothermal reaction, based on the strategy of synergistic modification by multiple functional groups. This compound features a novel 3D structure composed of 2D mercury tellurite layers bridged by phosphate tetrahedra. Excitingly, $Hg_2(HTe_2O_5)(PO_4)$ exhibits good optical properties. It has a large birefringence of 0.162 at 546 nm and 0.147 at 1064 nm, a band gap of 3.58 eV, and thermal stability up to 300 °C. Additionally, it remains stable when exposed to air for up to six months. These characteristics make $Hg_2(HTe_2O_5)(PO_4)$ a promising candidate as a birefringent material. PAWED calculations have revealed that the large birefringence is a result of the synergistic effects between the HgO_7 unit (19.86%), PO_4 group (29.17%) and Te_2O_5 unit (47.40%). Our work not only introduces a new phosphate birefringent material but also provides a novel approach to enhance the birefringence of tetrahedral compounds. This method of synergistic modification by multiple functional groups may inspire the development of other high-performance birefringent materials.

Author contributions

Peng-Fei Li: investigation, formal analysis, writing – original draft. Chun-Li Hu: formal analysis, theoretical calculations. Bo Zhang: investigation. Jiang-Gao Mao: supervision, resources, funding acquisition. Fang Kong: conceptualization, project administration, writing – review & editing. All authors have given approval to the final version of the manuscript.

Data availability

The data that support the findings of this study are available in the ESI† of this article.

Conflicts of interest

There are no conflicts to declare.

Acknowledgements

This work was supported by the National Natural Science Foundation of China (Grant No.: 22475215 and 22031009), the Natural Science Foundation of Fujian Province (Grant No.: 2023J01216, 2024J010039) and the Self-deployment Project Research Program of Haixi Institutes, Chinese Academy of Sciences (No. CXZX-2022-GH06). We are grateful for the birefringence measurements provided by Dr Hongyuan Sha at FJIRSM.

References

1 M. D. Fan, G. D. Wu, L. L. Li, F. P. Yu, C. Wang, X. F. Cheng and X. Zhao, Single Crystal Growth and Phase Transition Mechanism of $KCsMoP_2O_9$ with Efficient Second Harmonic Generation via the Emerging Additional Periodic Phase Technology, *J. Mater. Chem. C*, 2023, **11**, 12550–12560.

2 P. F. Li, C. L. Hu, J. G. Mao and F. Kong, Old tree blossoms anew: Research progress on the structures and optical properties of ultraviolet selenites, *Coord. Chem. Rev.*, 2024, **517**, 216000.

3 M. Mutailipu, J. Li and S. Pan, Looking Back the Nonlinear Optical Crystals in a Functionalized Unit's Perspective, *Adv. Funct. Mater.*, 2024, 2419204, DOI: **10.1002/adfm.202419204**.

4 S. Chen, Z. Bai, X. Song, T. Ouyang, Y. Li, Q. Ding, H. Wang, W. Chen, J. Luo and S. Zhao, A HTO–Type Nonlinear Optical Fluorophosphate with Ultrawide Bandgap, *Small*, 2025, **21**, 2408191.

5 X. Dong, L. Huang and G. Zou, Rational Design and Controlled Synthesis of High-Performance Inorganic Short-Wave UV Nonlinear Optical Materials, *Acc. Chem. Res.*, 2024, **58**, 150–162.

6 H. Sha, D. Yang, Y. Shang, Z. Wang, R. Su, C. He, B. Su, X. Yang, X. Long and S. Pan, The Directional Design of the Quasi–Phase–Matching Short–Wave Ultraviolet Nonlinear Optical Crystal, *Laser Photonics Rev.*, 2024, **18**, 2400992.

7 J. Dang, D. Mei, Y. Wu and Z. Lin, A comprehensive survey on nonlinear optical phosphates: Role of multicoordinate groups, *Coord. Chem. Rev.*, 2021, **431**, 213692.

8 H. Sha, J. Xu, Z. Xiong, Z. Wang, R. Su, C. He, X. Yang, X. Long and Y. Liu, An Optimized $KBe_2BO_3F_2$-Like Structure: The Unity of Deep-Ultraviolet Transparency, Nonlinear Optical Property, and Ferroelectricity, *Adv. Opt. Mater.*, 2022, **10**, 2200228.

9 J. Chen, M. B. Xu, H. Y. Wu, J. Y. Wu and K. Z. Du, Halogen Bond Unlocks Ultra–High Birefringence, *Angew. Chem., Int. Ed.*, 2024, **63**, e202411503.

10 M. Liang, Y. Zhang, E. Izvarin, M. J. Waters, J. M. Rondinelli and P. S. Halasyamani, Metal Methanesulfonates with Mixed Anionic Groups with Large Band Gaps and Enhanced Birefringence, *Chem. Mater.*, 2024, **36**, 2113–2123.

11 H. Sha, D. Yang, Q. Li, L. Yang, Z. Wang, R. Su, C. He, B. Su, X. Yang and X. Long, Designing a Heteroleptic Tetrahedral Group with an Ultrahigh Polarizability Anisotropy by Optimizing the Bonding Electrons Activity and Their Distribution, *Laser Photonics Rev.*, 2025, **19**, 2401785.

12 B. Zhang, M. Y. Ran, X. T. Wu, H. Lin and Q. L. Zhu, Recent advances and future perspectives on rare-earth-based nonlinear optical materials with π-conjugated $[XO_3]$ (X = B, C, N) units, *Coord. Chem. Rev.*, 2024, **517**, 216053.

13 R. Wei, H. Huang, D. Yang, Y. Wang and B. Zhang, $C_6N_7(NH_2)_3{\cdot}H_3PO_4$: Strong Second Harmonic Generation

and Giant Birefringence Benefiting from Amino Substitution Strategy, *Adv. Opt. Mater.*, 2024, **12**, 2401814.

14 Z. Li, C. Jin, C. Liu, J. Lu, Z. Yang, S. Pan and M. Mutailipu, $[B_3O_3F_4(OH)]^{2-}$: A Versatile Hydroxyfluorooxoborate Heteroanion Producing Compounds with Highly Tunable Optical Anisotropy, *Chem. Mater.*, 2024, **36**, 6985–6993.

15 H. Cheng, M. Cheng, A. Tudi and X. Hou, $K_2PbB_5P_3O_{17}$: A Mixed-Coordinated Borophosphate with Enhanced Birefringence Driven by the $[B_2O_5]$ Unit, *Inorg. Chem.*, 2025, **64**, 4393–4398.

16 H. N. Liu, H. P. Wu, Z. G. Hu, J. Y. Wang, Y. C. Wu and H. W. Yu, $Cs_3[(BOP)_3(B_3O_7)_3]$: A Deep-Ultraviolet Nonlinear Optical Crystal Designed by Optimizing Matching of Cation and Anion Groups, *J. Am. Chem. Soc.*, 2023, **145**, 12691–12700.

17 Y. Hou, B. Zhang, H. Wu, H. Yu, Z. Hu, J. Wang and Y. Wu, $K_3B_4PO_{10}$ and $K_2MB_4PO_{10}$ (M = Rb/Cs): rare mixed-coordinated borophosphates with large birefringence, *Inorg. Chem. Front.*, 2021, **8**, 1468–1475.

18 B. Cheng, Z. Li, Y. Chu, A. Tudi, M. Mutailipu, F. Zhang, Z. Yang and S. Pan, $(NH_4)_3B_{11}PO_{19}F_3$: a deep-UV nonlinear optical crystal with unique $[B_5PO_{10}F]_\infty$ layers, *Natl. Sci. Rev.*, 2022, **9**, nwac110.

19 Y. Li and K. M. Ok, Breaking Boundaries: Giant Ultraviolet Birefringence in Dimension–Reduced Zn–Based Crystals, *Angew. Chem., Int. Ed.*, 2024, **63**, e202409336.

20 J. Chen, H. Y. Wu, M. B. Xu, M. C. Wang, Q. Q. Chen, B. X. Li, C. L. Hu and K. Du, Halide-Driven Polarity Tuning and Optimized SHG-Bandgap Balance in $(C_4H_{11}N_2)ZnX_3$ (X = Cl, Br, I), *Inorg. Chem. Front.*, 2024, **11**, 5587–5597.

21 Z. Fang, C. Q. Li, B. P. Yang and M. H. Duan, Na $(C_2H_{10}N_2)_2[Zn_3(PO_4)_2(H_{0.5}PO_4)]_2$: A Short-Wave Ultraviolet Open-Framework Zincophosphate Exhibiting Substantial Optical Dispersion Ability, *Inorg. Chem.*, 2024, **63**, 18547–18551.

22 Y. L. Sun, G. X. Liu, Y. L. Lv, L. Ma, W. D. Yao and R. L. Tang, $(NH_4)_3(H_3O)Zn_4(PO_4)_4$: A nonlinear optical zinc orthophosphate crystal, *J. Solid State Chem.*, 2023, **325**, 124171.

23 B. L. Wu, C. L. Hu, F. F. Mao, R. L. Tang and J. G. Mao, Highly Polarizable Hg^{2+} Induced a Strong Second Harmonic Generation Signal and Large Birefringence in $LiHgPO_4$, *J. Am. Chem. Soc.*, 2019, **141**, 10188–10192.

24 C. Deng, X. Xu, Y. Y. Hu, J. Y. Guo, L. M. Wu and L. Chen, Tin Chalcohalide $Sn_{11}(PS_4)_4I_{10}$ Obtained by Structural-template-oriented Synthesis: Exhibiting Balanced Infrared Nonlinear Optical Performance, *Inorg. Chem. Front.*, 2025, **12**, 1437–1443.

25 S. J. Han, A. Tudi, W. B. Zhang, X. L. Hou, Z. H. Yang and S. L. Pan, Recent Development of Sn(II), Sb(III)-based Birefringent Material: Crystal Chemistry and Investigation of Birefringence, *Angew. Chem., Int. Ed.*, 2023, **62**, e202302025.

26 J. Y. Guo, J. B. Huang, A. Tudi, X. L. Hou, S. J. Han, Z. H. Yang and S. L. Pan, Birefringence Regulation by Clarifying the Relationship Between Stereochemically Active Lone Pairs and Optical Anisotropy in Tin-based Ternary Halides, *Angew. Chem., Int. Ed.*, 2023, **62**, e202304238.

27 J. Y. Guo, S. C. Cheng, S. J. Han, Z. H. Yang and S. L. Pan, $Sn_2B_5O_9Br$ as an Outstanding Bifunctional Material with Strong Second-Harmonic Generation Effect and Large Birefringence, *Adv. Opt. Mater.*, 2021, **9**, 2001734.

28 P. F. Li, Y. P. Gong, C. L. Hu, B. Zhang, J. G. Mao and F. Kong, Four UV Transparent Linear and Nonlinear Optical Materials Explored from Pure Selenite Compounds, *Adv. Opt. Mater.*, 2024, **12**, 2301426.

29 Z. Fang, W. H. Ma, Q. Y. Chen, X. T. Zhu, X. M. Zeng, P. B. Li, Q. F. Zhou, T. T. Song and M. H. Duan, From $(NH_4)_3[Zr(PO_4)_2F]$ to $(NH_4)_3[Sn_2(PO_4)_2]Cl$: Rational Design of a Tin-based Short-Wave Ultraviolet Phosphate with Large Optical Anisotropy, *Inorg. Chem. Front.*, 2024, **11**, 1775–1780.

30 M. Hu, J. Wang, N. Tuerhong, Z. Zhang, Q. Jing, Z. Chen, Y. L. Yang and M.-H. Lee, Novel Antimony Phosphates with Enlarged Birefringence Induced by Lone Pair Cations, *Dalton Trans.*, 2024, **53**, 3377–3385.

31 Y. Y. Hu, X. Xu, R. X. Wang, J. Y. Han, S. S. Zhang, S. H. Zhang, J. Y. Guo, L. M. Wu and L. Chen, $[Sn_3OF]PO_4$ vs $[Sn_3F_3]PO_4$: Enhancing Birefringence through Breaking *R*3 Symmetry and Realigning Lone Pairs, *Inorg. Chem. Front.*, 2024, **11**, 5648–5656.

32 L. Deng, R. Zhang, J. Zhang, W. Xie, C. Bai, Z. Yang, X. Hou, S. Han and S. Pan, Stereochemically Active Tin(II) Induced Enhancement of Birefringence in Sn(II)Sn(IV) $(PO_4)_2$ and $SrSn(PO_4)PO_2(OH)_2$, *Chem. Eur. J.*, 2023, **29**, e202300743.

33 J. Guo, A. Tudi, S. Han, Z. Yang and S. Pan, Sn_2PO_4I: An Excellent Birefringent Material with Giant Optical Anisotropy in Non pi-Conjugated Phosphate, *Angew. Chem., Int. Ed.*, 2021, **60**, 24901–24904.

34 M. Zhao, Y. Sun, Y. Wu, D. Mei, S. Wen and T. Doert, $NaTePO_5$, $SrTeP_2O_8$ and $Ba_2TeP_2O_9$: Three tellurite-phosphates with large birefringence, *J. Alloys Compd.*, 2021, **854**, 157243.

35 X. H. Dong, H. B. Huang, L. Huang, Y. Q. Zhou, B. B. Zhang, H. M. Zeng, Z. E. Lin and G. H. Zou, Unearthing Superior Inorganic UV Second–Order Nonlinear Optical Materials: A Mineral–Inspired Method Integrating First–Principles High–Throughput Screening and Crystal Engineering, *Angew. Chem., Int. Ed.*, 2024, **63**, e202318976.

36 C. Hu, X. Cai, M. Wu, Z. Yang, J. Han and S. Pan, Lone Pair-Driven Enhancement of Birefringence in Polar Alkali Metal Antimony Phosphates, *Chem. Mater.*, 2022, **34**, 4224–4231.

37 S. Liu, C. Li, J. Jiao, Y. She, T. Zhang, D. Ju, N. Ye, Z. Hu and Y. Wu, Three In One: A Cadmium Bismuth Vanadate NLO Crystal Exhibiting a Large Second-Harmonic Generation Response and Enhanced Birefringence, *Inorg. Chem. Front.*, 2024, **11**, 2384–2391.

38 J. H. Wu, C. L. Hu, T. K. Jiang, J. G. Mao and F. Kong, Highly Birefringent d^0 Transition Metal Fluoroantimonite in the Mid Infrared Band: Order–Disorder Regulation by Cationic Size, *J. Am. Chem. Soc.*, 2023, **145**, 24416–24424.

39 Y. Zhang, M. H. Lv, S. F. Li, H. Huang, B. Zhang and D. Yan, $[C(NH_2)_3]_{10}(MoO_3)_{10}(PO_4)_2(HPO_4)_2{\cdot}5H_2O$: Synergy effect of multiple functional units results in significant birefringence, *J. Solid State Chem.*, 2024, **337**, 124823.

40 K. Hou, C. Liu, Q. Feng, Y. Yang and B. Zhang, Enhanced Birefringence in Phosphates via "Two Steps in One": d0 Transition Metal Regulation and Fluorination Synergistic Strategy, *J. Phys. Chem. C*, 2024, **128**, 7352–7358.

41 Z. Gao, Q. Feng, J. Lu and H. Du, $K_2MgMoP_2O_{10}$ and $K_3Mg_2MoP_3O_{14}$: two new molybdophosphates exhibiting different optical anisotropy induced by variable dimensionality of the anion framework, *Dalton Trans.*, 2024, **53**, 10686–10692.

42 P. F. Li, C. L. Hu, B. X. Li, J. G. Mao and F. Kong, $Hg_3Se(SeO_3)(SO_4)$: A Mixed-Valent Selenium Compound with Mid-Infrared Transmittance Obtained by In Situ Reaction, *Inorg. Chem.*, 2024, **63**, 4011–4016.

43 M. S. Zhang, W. D. Yao, S. M. Pei, B. W. Liu, X. M. Jiang and G. C. Guo, $HgBr_2$: An Easily Growing Wide-Spectrum Birefringent Crystal, *Chem. Sci.*, 2024, **15**, 6891–6896.

44 X. H. Dong, L. Huang, H. M. Zeng, Z. E. Lin, K. M. Ok and G. H. Zou, High-Performance Sulfate Optical Materials Exhibiting Giant Second Harmonic Generation and Large Birefringence, *Angew. Chem., Int. Ed.*, 2022, **61**, e202116790.

45 R. L. Tang, Y. L. Lv, L. Ma, B. W. Miao, W. L. Liu and S. P. Guo, "All-Four-in-One": A Novel Mercury Tellurite-Nitrate $Hg_3(TeO_3)(Te_3O_7)(NO_3)_2$ Exhibiting Exceptional Optical Anisotropy, *Chem. Sci.*, 2025, **16**, 4749–4754.

46 T. Wu, X. Jiang, K. Duanmu, C. Wu, Z. Lin, Z. Huang, M. G. Humphrey and C. Zhang, Giant Optical Anisotropy in a Covalent Molybdenum Tellurite via Oxyanion Polymerization, *Adv. Sci.*, 2024, **23**, 2306670.

47 Y. Ding, M. Zhu, J. Wang, B. Li, H. Qi, L. Liu and Y. Chu, $Pb_2TeV_2O_{10}$: A Lead Vanadate Tellurate with Wide Mid-IR Transparency and Large Birefringence Induced by Multiple Birefringence-Active Groups, *Inorg. Chem.*, 2024, **63**, 20003–20013.

48 T. Zhang, J. Jiao, W. Zhao, F. Wang, F. Liang, N. Ye, Z. Hu, Y. Wu and C. Li, Rational Design of a Niobium Tellurite Crystal $Nb_2Te_3O_{11}$ Exhibiting Good Overall Infrared NLO Performance by Structural Genetic Engineering, *Inorg. Chem.*, 2023, **62**, 17522–17529.

49 P. F. Li, C. L. Hu, Y. F. Li, J. G. Mao and F. Kong, $Hg_4(Te_2O_5)(SO_4)$: A Giant Birefringent Sulfate Crystal Triggered by a Highly Selective Cation, *J. Am. Chem. Soc.*, 2024, **146**, 7868–7874.

50 P. F. Li, C. L. Hu, J. G. Mao and F. Kong, A Giant Optically Anisotropic Phosphate Driven by Mixed Valence Mercury Units, *Laser Photonics Rev.*, 2025, **19**, 2401488.

51 L. Ma, Y. L. Lv, X. F. Ao, W. Liu, S. P. Guo and R. L. Tang, Centric $Sc(HPO_3)(H_2PO_3)(H_2O)$ and Acentric $Sc(H_2PO_3)_3$: Two Ultraviolet Scandium Phosphite Optical Crystals, *Inorg. Chem.*, 2024, **63**, 7118–7122.

52 Y. She, J. Jiao, Z. Wang, J. Chai, S. Jie, N. Ye, Z. Hu, Y. Wu and C. Li, $LiVTeO_5$: a mid-infrared nonlinear optical vanadium tellurate crystal exhibiting enhanced second harmonic generation activities and notable birefringence, *Inorg. Chem. Front.*, 2023, **10**, 6557–6565.

53 Q. Wu, J. Zhou, X. Liu, X. Jiang, Q. Zhang, Z. Lin and M. Xia, $Ca_3(TeO_3)_2(MO_4)$ (M = Mo, W): Mid-Infrared Nonlinear Optical Tellurates with Ultrawide Transparency Ranges and Superhigh Laser-Induced Damage Thresholds, *Inorg. Chem.*, 2021, **60**, 18512–18520.

54 P. F. Li, C. L. Hu, B. X. Li, J. G. Mao and F. Kong, From $CdPb_8(SeO_3)_4Br_{10}$ to $Pb_3(TeO_3)Br_4$: The first tellurite bromide exhibiting SHG response and mid-IR transparency, *Inorg. Chem. Front.*, 2023, **10**, 7343–7350.

55 P. F. Li, C. L. Hu, J. G. Mao and F. Kong, $Hg_2(SeO_3)(TeO_3)$: A novel tellurite-selenite birefringent crystal achieved by assembling multiple functional groups, *J. Mater. Chem. C*, 2025, **13**, 4374–4378.

56 J. Ren, H. Cui, L. Cheng, Y. Zhou, X. Dong, D. Gao, L. Huang, L. Cao and N. Ye, $A_2Hg_x(SeO_3)_y$ (A = K, Rb, Cs): Three Alkali Metal Mercury Selenites Featuring Unique 1D $[HgO_m(SeO_3)_n]_\infty$ Chains, *Inorg. Chem.*, 2023, **62**, 21173–21180.

57 P. F. Li, C. L. Hu, Y. P. Gong, F. Kong and J. G. Mao, $Hg_3(Te_3O_8)(SO_4)$: a new sulfate tellurite with a novel structure and large birefringence explored from d^{10} metal compounds, *Chem. Commun.*, 2021, **57**, 7039–7042.

58 P. F. Li, C. L. Hu, B. Zhang, J. G. Mao and F. Kong, From $HgGa_2(SeO_3)_4$ to $Hg_2Ga(SeO_3)_2F$: the first Hg^I-based selenite birefringent crystal triggered by linear groups and fluoride ions, *Chin. Chem. Lett.*, 2024, 110588, DOI: **10.1016/j.cclet.2024.110588**.

59 H. Sha, D. Yang, Y. Shang, Z. Wang, R. Su, C. He, X. Yang and X. Long, Trithionic guanidine: A novel semi-organic short-wave ultraviolet nonlinear optical sulfate with dimeric heteroleptic tetrahedra, *Chin. Chem. Lett.*, 2024, 109730, DOI: **10.1016/j.cclet.2024.109730**.

60 P. F. Li, C. L. Hu, F. Kong and J. G. Mao, The First UV Nonlinear Optical Selenite Material: Fluorination Control in $CaYF(SeO_3)_2$ and $Y_3F(SeO_3)_4$, *Angew. Chem., Int. Ed.*, 2023, **62**, e202301420.

61 B. Zhang, S. Zhou, B. X. Li, X. Wu, H. Lin and Q. L. Zhu, Exploring New Horizons in Mid-to-Far Infrared Nonlinear Optical Crystals: The Significant Potential of Trigonal Pyramidal $[TeS_3]^{2-}$ Functional Units, *Chem. Sci.*, 2025, **16**, 3218–3227.

62 M. Y. Ran, S. H. Zhou, B. X. Li, X. T. Wu, H. Lin and Q. L. Zhu, Balanced IR Nonlinear Optical Performance Achieved by Cation–Anion Module Cosubstitution in V-Based Salt-Inclusion Oxychalcogenides, *Chem. Mater.*, 2024, **36**, 11996–12005.

63 P. F. Li, C. L. Hu, J. G. Mao and F. Kong, A UV non-hydrogen pure selenite nonlinear optical material for achieving

balanced properties through framework-optimized structural transformation, *Mater. Horiz.*, 2024, **11**, 1704–1709.
64 G. Ghosh, Dispersion-equation coefficients for the refractive index and birefringence of calcite and quartz crystals, *Opt. Commun.*, 1999, **163**, 95–102.
65 X. Shi, X. Liu, C. Nie, Y. Zhang, D. Zhong, B. Teng, Z. Lin, Y. Huang and S. Sun, $SnHPO_4$: A Layered Tin(II) Phosphate with Enhanced Birefringence, *Inorg. Chem.*, 2025, **64**, 2127–2132.
66 J. Guo, X. Zhan, J. Lan, X. Liu, S. Zhao, X. Xu, L.-M. Wu and L. Chen, $Sb_4O_5I_2$: Enhancing Birefringence through Optimization of Sb/I Ratio for Alignment of Stereochemically Active Lone Pairs, *Inorg. Chem.*, 2024, **63**, 2217–2223.
67 X. Y. Li, X. Y. Cheng, C. L. Hu, B. X. Li, Z. Y. Zhou, J. H. Zhang, S. Q. Deng, J. G. Mao and F. Kong, From Holodirected to Hemidirected Coordination Activated by Oxygenation Strategy: A Facile Route to Long Wave Infrared Birefringent Crystal, *Angew. Chem., Int. Ed.*, 2025, e202501481, DOI: **10.1002/anie.202501481**.
68 P. F. Li, C. L. Hu, F. Kong and J. G. Mao, $AAl(Te_4O_{10})$ (A = Na, Ag) and $K_2Ga_2(HTe_6O_{16})(HTeO_3)$: Three Aluminum/Gallium Tellurites with Large Birefringence and Wide Band Gap, *Inorg. Chem.*, 2023, **62**, 8494–8499.
69 Q. Q. Chen, C. L. Hu, M. Z. Zhang and J. G. Mao, $(C_5H_{6.16}N_2Cl_{0.84})(IO_2Cl_2)$: A Birefringent Crystal Featuring Unprecedented $(IO_2Cl_2)^-$ Anions and π-Conjugated Organic Cations, *Chem. Sci.*, 2023, **14**, 14302–14307.